

# Modeling the Water Circulation in the North Atlantic in the Scope of the CORE-II Experiment

K. V. Ushakov<sup>a, b, c</sup>, T. B. Grankina<sup>b, c</sup>, and R. A. Ibraev<sup>a, b, c, d</sup>

<sup>a</sup>*Institute of Numerical Mathematics, Russian Academy of Sciences, ul. Gubkina 8, Moscow, 119333 Russia*

<sup>b</sup>*Shirshov Institute of Oceanology, Russian Academy of Sciences, Nakhimovskii pr. 36, Moscow, 117997 Russia*

<sup>c</sup>*Hydrometeorological Center of the Russian Federation, Bol'shoi Predtechenskii per. 11-13, Moscow, 123242 Russia*

<sup>d</sup>*Moscow Institute of Physics and Technology, Institutskii per. 9, Dolgoprudnyi, Moscow oblast, 141700 Russia*

*e-mail: ushakovkv@mail.ru*

Received December 22, 2015

**Abstract**—A numerical experiment on the reproduction of the variability in the state of North Atlantic water in 1948–2007 with a spatial resolution of  $0.25^\circ$  has been performed using the global ocean model developed at Institute of Numerical Mathematics, Russian Academy of Sciences (INM RAS), and the Shirshov Institute of Oceanology (IO RAS) (the INM–IO model). The data on the state of the atmosphere, radiation fluxes, and bulk formulas of the CORE-II protocol are used as boundary conditions. Five successive 60-year calculation cycles have been performed in order to obtain the quasi-equilibrium state of a model ocean. For the last 20 years, the main elements of large-scale ocean circulation have been analyzed and compared with the WOA09 atlas data and the results of other models.

**Keywords:** the North Atlantic, climate, ocean numerical simulation, CORE-II experiment

**DOI:** 10.1134/S0001433816040113

## 1. INTRODUCTION

It is necessary to understand many complex poorly studied physical processes in different mediums (water, ice, and the atmospheric boundary layer) in order to solve current oceanological problems, which cannot be performed without using mathematical simulation. The large volume of data and ambiguous parametrization of these processes make it especially difficult to model the ocean and the entire climatic system of the Earth. To improve models, it is necessary to verify them based on observational data and compare them with the results of other models, which in turn makes it possible to better understand the physical mechanisms responsible for the state of a real ocean [1, 2].

Using the INM–IO numerical model [3], we calculated the variations in the World Ocean water circulation and the sea ice state from 1948 to 2007. The experimental set up corresponds to the CORE-II protocol [4, 5], according to which the calculations are performed by research teams in different states and are aimed at a coordinated study of different regions and physical characteristics of the World Ocean. The present work contributes to one such direction proposed in [6], namely, studying the present-day state of the North Atlantic ocean basin and the role of the Atlantic meridional overturning circulation. We analyze the calculation results averaged over the last 20 years,

comparing them with the data of the WOA09 climatic atlas [7] and with the results for several models presented in [6]. This work continues the study [8], which considered the quasi-stationary state of the World Ocean obtained after 500 years of the model integration with recurrent “normal” year forcing of the CORE-I atmospheric data. In Russia works on this subject matter have also been performed by the research team of the INMOM model, which substantially differs from the INM–IO in the set of applied numerical algorithms [6, 9].

In Section 2 we describe the INM–IO model, its configurations, and the set up of the numerical experiment. In Section 3 we analyze the calculation results and compare them with the data of WOA09 and other models. Section 4 presents the conclusions and specifies the planned aspects of a further work.

## 2. INM–IO MODEL AND NUMERICAL EXPERIMENT SET UP

The INM–IO numerical model of the World Ocean was developed in order to study the seawater circulation in a wide range of spatial and time scales. The primitive system of equations for the 3D ocean dynamics in Boussinesq and hydrostatic approximations [10] was approximated by the finite volume method on the B-type grid in vertical  $z$  coordinates.

The horizontal grid is tripolar with a resolution of  $0.25^\circ$  in the spherical part. The vertical discretization includes 49 horizons spaced at 6 m in the upper layer to 250 m at larger depths. The time step is 10 min for baroclinic processes. We calculated independently a fast barotropic dynamics by solving the system of shallow-water equations with a step of 25 s. We apply an original fast algorithm [11] for solving the system of shallow-water equations using parallel distributed-memory computers.

The state of sea ice is described by the thermodynamic model [12]. We described the air–water interface together with the fluxes of heat, momentum, and water using the CORE bulk formulas [4]. By temperature we mean the potential temperature relative to the ocean surface. The condition of free sliding is used at solid boundaries. Biharmonic filters are used to additionally maintain the numerical stability in the equations of momentum, temperature, and salinity transport. The variable horizontal diffusion coefficient was taken proportional to the minimal grid step at a given point, and the biharmonic diffusion coefficient is proportional to the third degree of the step. The corresponding values at the equator are  $1000 \text{ m}^2 \text{ s}^{-1}$  and  $-2.8 \times 10^{11} \text{ m}^4 \text{ s}^{-1}$ . The horizontal viscosity coefficient is specified according to the Smagorinsky method with a factor of  $C^2 = 2.5^2$  [13]. The background value at the equator is  $2060 \text{ m}^2 \text{ s}^{-1}$ . For biharmonic viscosity, the factor is 1 and the background field is zero. The indicated values of the viscosity and diffusion coefficients (not biharmonic) correspond to the analyzed calculation cycle (see below in this section). The coefficients larger by factors of 1.4 and 2.8 were taken in the previous cycles. A viscosity coefficient of  $300 \text{ m}^2 \text{ s}^{-1}$  is used in the shallow-water equation.

To calculate the momentum transport, we applied the central difference scheme; to calculate the heat and salt transport we applied the scheme with the correction of fluxes. Vertical mixing is parametrized according to the Munk–Anderson scheme, including a convective adjustment. The background values of vertical viscosity and diffusion are  $10^{-4}$  and  $10^{-6} \text{ m}^2 \text{ s}^{-1}$ , and the maximal values in the regions with a small Richardson number are  $10^{-2}$  and  $10^{-3} \text{ m}^2 \text{ s}^{-1}$ , respectively. All processes except vertical turbulent mixing are described by the explicit numerical methods, which made it possible to effectively parallelize the software code. The model was implemented on massive parallel computers controlled by the Compact modelling framework [14], maintaining parallel exchanges, multilevel data interpolation, and asynchronous operation with the file system. The model is described in more detail in [3].

The experimental set up corresponds to the CORE-II protocol, specifying the daily mean descending radiation fluxes, monthly mean precipitation, and river flow, as well as the daily variations in the atmospheric parameters (temperature, humidity, and wind velocity at an altitude of 10 m) during a

60-year period (1948–2007) according to the reanalysis data and satellite observations. The data include several modifications [4, 15] that are used to provide for the thermal balance of the ocean model, which operates without a complete model of the atmosphere. To form the quasi-equilibrium state of the solution, we perform the calculation for 300 years (five 60-year cycles without interruption) with a jump in going from conditions for 2007 to conditions for 1948.

To avoid drift, we relax the surface salinity to a modified monthly mean climatic field using an artificial salt flux proportional to the local salinity anomaly with a coefficient of 50 m per four years (weak relaxation according to [4]). On the ocean surface we apply the normalization (the subtraction of the average global value) for the water flux and the artificial salt flux. The initial temperature and salinity fields were taken equal to the mean annual WOA09 fields, and the initial values of the current velocities and the sea ice thickness are zero. Inland basins and the Black Sea are ignored in the calculations.

A comparison of the results with the model data [6], obtained under the same atmospheric conditions and using the same bulk formulas, allows us to make an assumption about the origination of deviations of the model solution from observations and prepare the basis for studying the variations in the ocean state on different timescales.

### 3. EXPERIMENTAL RESULTS

We consider the North Atlantic region as the first stage of studies according to the CORE-II program using the INM–IO model and analyze the present-day state of the region reproduced by the model. As in [6], we will consider the fields averaged for the last 20 years in the fifth cycle of the experiment (corresponding to the external conditions in 1988–2007) unless otherwise specified, and will compare these fields with the mean annual climatic data from the WOA09 atlas.

#### 3.1. Atlantic Meridional Circulation

The climate of the North Atlantic largely depends on the heat and salt flows transferred by the meridional overturning circulation (MOC) of water; therefore, it is important to correctly reproduce the circulation intensity in order to realistically model the region. According to [4], this value was very sensitive to the parameter setting of the model. A low MOC intensity can result from an excessive viscosity of the model ocean.

Figure 1 shows the distribution of the Atlantic MOC streamfunction constructed based on the average velocity field obtained by us. The function value at a plot point is equal to the southward integral water transport at a given latitude through the vertical section from the bottom to a given depth. The maximums

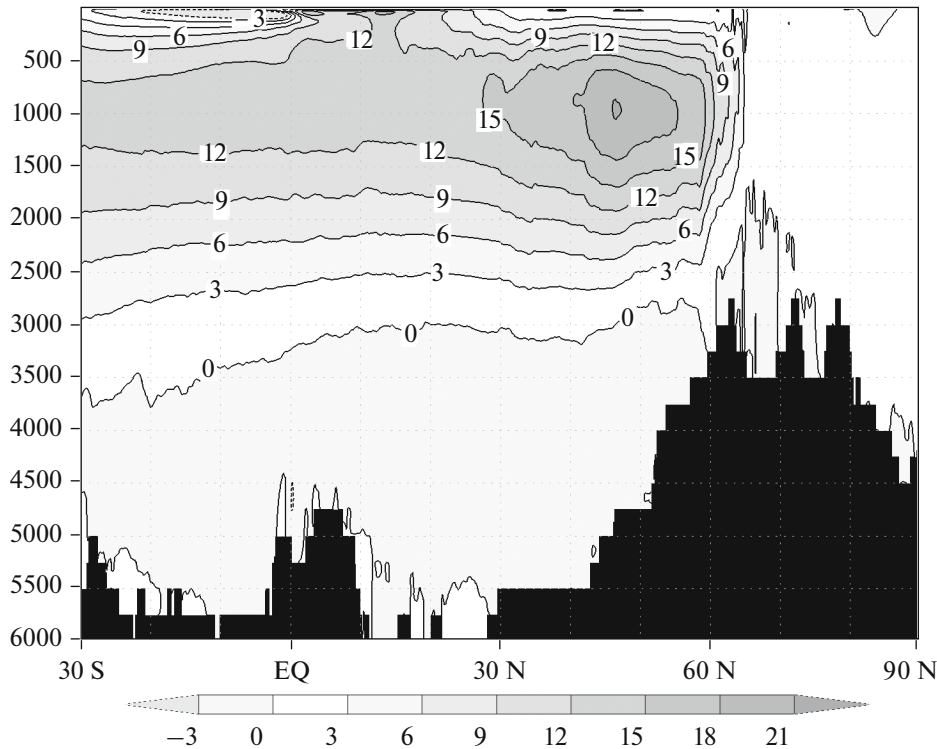


Fig. 1. Atlantic MOC streamfunction according to the calculation performed using the INM-IO model.

correspond to the circulation centers in a clockwise direction. The function primary maximum is about 21 Sv, which falls in the upper part of the result scatter of a low-resolution model [6] (8–28 Sv) and exceeds the data obtained in [16] with the  $0.25^\circ$  (18 Sv), [17]  $0.1^\circ$  (17.4 Sv), and [18]  $(1/12)^\circ$  (18 Sv) resolutions. The maximum location depths are close in different works (about 900–1100 m), whereas the latitudes differ pronouncedly:  $45^\circ$  N in our work,  $30^\circ$ – $55^\circ$  N in [6], and  $30^\circ$ – $35^\circ$  N in [16–18]. This difference should be studied independently, but a comparison of the sources of literature indicates that the maximum point as a rule shifts southward as the model resolution increases. Comparing the results of the experiment and works [4, 6, 8], we can assume that the maximum shifts northward because the mixing depths are increased in the Labrador Sea and the Irminger Basin (see Fig. 7).

The penetration depth of the North Atlantic deep water (NADW), determined based on the streamfunction zero isoline, is about 3000 m in our case, which coincides with most models in [6] but is smaller than the available measurement data. In Fig. 2 the Atlantic MOC vertical profile at  $26.5^\circ$  N latitude is compared based on the INM-IO and [6] data. The estimation based on the observational data according to the RAPID program, taken from the same work, is also presented. In contrast to Fig. 1, the streamfunction for all model data is specified here as an integral northward water transport between the surface and the selected depth. Therefore, the function at the bottom

can differ from zero, which corresponds to the contribution of the current through the Bering Strait and water fluxes on the ocean surface to MOC. In the RAPID data, the correction constant in space, such as the streamfunction at the bottom is zero, is added to the flow field. The average data for April 2004 to March 2008 is used; therefore, the 4-year average for the next available years (2004–2007) is also taken for the models. Despite the fact that the RAPID estimation is uncertain (the velocity field is corrected and the reference level method is used to calculate MOC at open ocean depths [19, 20]), we can rather confidently state that the INM-IO model, as well as most remaining models (see Fig. 5 in [6]), underestimates the meridional water transport (10–15 Sv in the models and 18.6 Sv in the RAPID data). The NADW penetration depth is insufficiently large, and, correspondingly, the Antarctic bottom water occupies a wider range of depths (from 2500–3000 m to the bottom in most models and from 4400 m in the RAPID data). The water southward transport maximum for the INM-IO model (4.2 Sv at a depth of 3.5 km) lies near the upper boundary of the model scatter [6].

Since NADW is mainly replenished by cold and dense water of Nordic seas flowing through the Greenland–Scotland Ridge [21], it is apparently necessary to parametrize the process in order to improve the reproduction of this water. The NCAR model in [6], which uses such a parametrization, indicated a depth close to the observations.

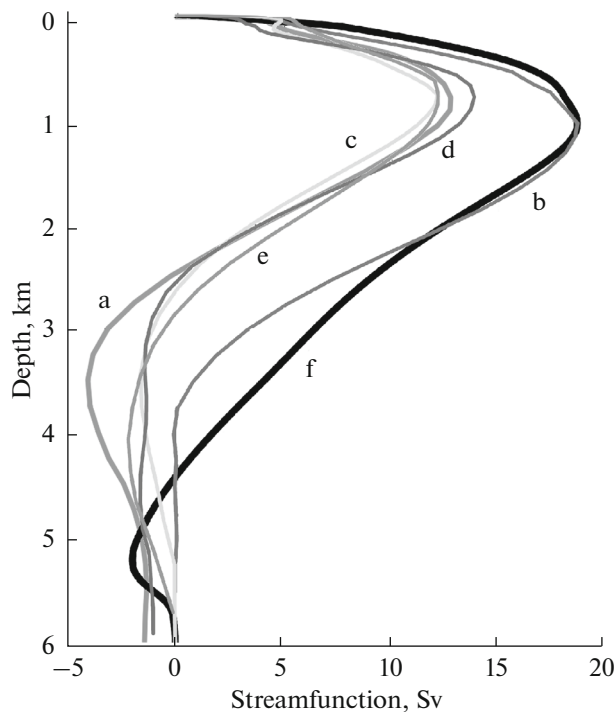


**Fig. 2.** Vertical profile of the Atlantic MOC streamfunction at  $26.5^\circ$  N latitude according to the data of (a) the INM–IO model and some models from [6] (b) NCAR, (c) MIT, (d) AWI, and (e) MRI-F) and (f) the estimation made using the RAPID program data.

### 3.2. Meridional Heat Transport

The meridional heat transport (MHT) by the ocean from tropical latitudes to polar regions is important in the formation of the Earth's climate. Figure 3 presents the latitude distribution of the Atlantic MHT according to the results of our experiment as compared to the data from [6]: the results of some models, the implicit MHT calculation in [15] based on the climatology of the atmospheric and ocean surface data for 1984–2006, and the estimates based on the data of measurements from [22, 23].

For INM–IO, we calculated MHT as a sum of advection and diffusion heat fluxes calculated immediately according to the model numerical schemes. The result is generally close to the estimates based on the observations and is near the uncertainty lower boundary, whereas most 18 models in [6] show smaller MHT values. All models failed to reproduce the estimation based on the RAPID data [23]. The authors of [24] indicated that decreased model MHT values at realistic (or even increased) MOC values are possibly caused by a diffused thermocline and an insufficient NADW penetration depth.

If the model reaches the state of equilibrium, the positive (negative) graph slope indicates ocean integral heating (cooling) through the surface at a correspond-

ing latitude. Thus, the graph slope is positive near  $45^\circ$ – $55^\circ$  N due to the atmospheric heat flux, which tends to suppress a decrease in the surface temperature that is observed in most considered models since the North Atlantic current route is too zonal (Fig. 4). At about  $65^\circ$  N, the INM–IO graph spike is apparently caused by an increased flow rate of a cold East Greenland current (subsection 3.3).

### 3.3. Temperature and Salinity

Temperature and salinity distributions make it possible to judge model circulation singularities, specifically, the quality of reproduction of currents, vertical mixing, and water mass formation. Based on the INM–IO model results, we consider the temperature and salinity deviations from the WOA09 atlas data, averaged over the depth of the upper 700-m layer (Fig. 4) and over latitude (Fig. 5). The dashed isolines correspond to the negative values.

The temperature and salinity deviations often compensate each other to a certain degree in the density field. This is illustrated by warm and saline water near the North American coast and by cold freshened water at midlatitudes in the Atlantic Ocean, which is also present in many models [6]. This indicates that the point of the Gulf Stream separation from the continental slope shifts northward in the model solution and the North Atlantic current is zonal in the region of the Subpolar gyre.

Extensive freshening in the Greenland Sea is probably caused by increased ice formation during winter (Fig. 6) and the following increased flux of fresh melt water in summer. Fresh water blocks vertical mixing, which is seen in the model solution as a warming at depths of 500–2000 m in this region. A similar effect was obtained in [6] using the ICTP model, according to which the Atlantic MOC maximum is shifted northward like in the INM–IO model.

In the  $60^\circ$  N region, vertical mixing is on the contrary intense, which is shown as a descent of warm and saline Atlantic water. The velocity of the East Greenland Current south of the Denmark Strait is increased: the mean annual values constantly reach  $20$ – $30$   $\text{cm s}^{-1}$  on the shelf slope to the sill depths. The total average flow rate through the strait for 20 years is  $5.8$  Sv, whereas this flow rate is  $3$ – $4$  Sv according to the measurements and eddy-resolving models [25]. As a result, cold and fresh water erroneously originates south of the strait. Warm and saline water, extending along the northwestern African coast and through the tropical Atlantic to depths of  $1000$ – $2000$  m, was typical of the INM–IO model and, to a certain degree, of most models in [4, 6]. This can indicate that the model resolution is insufficient for the reproduction of upwelling, and the atmospheric or oceanic (climatic) data in the tropics include errors.

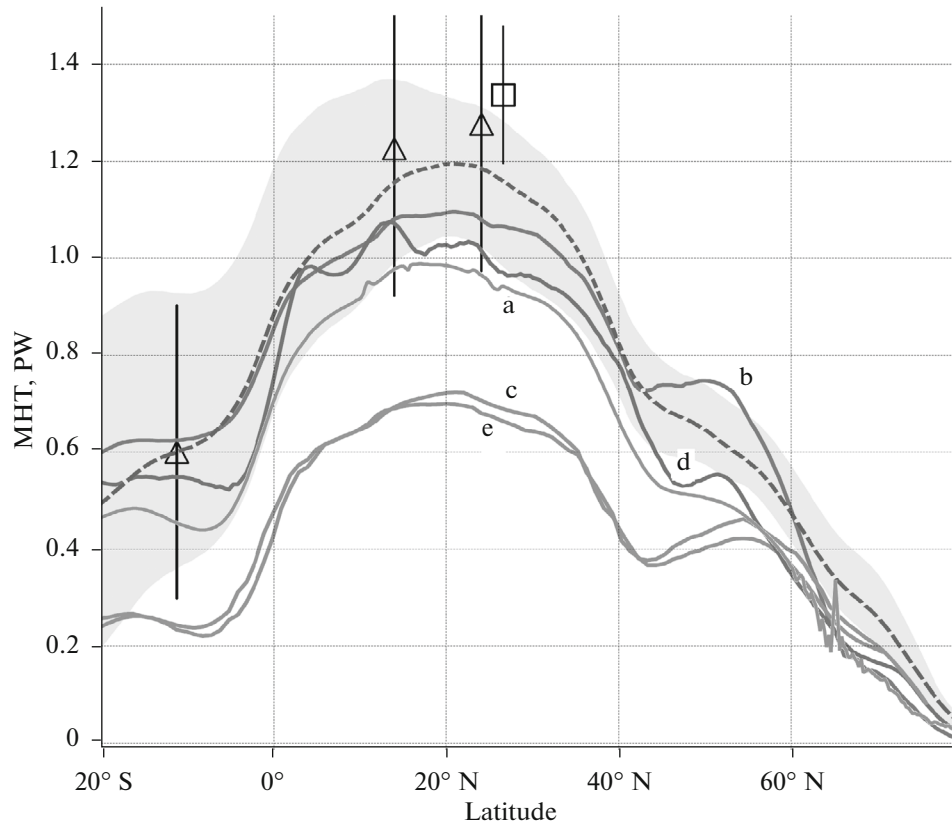


**Fig. 3.** Meridional heat transport in the Atlantic Ocean according to the data of the INM–IO model, models from [6] ((b) NCAR, (c) MIT, (d) AWI, and (e) MRI-F), and estimates from [22, 23] (triangles and a square, respectively, with uncertainty intervals), and calculations performed in [15] with the variability range for 1984–2006 (a dashed line and a filled region).

**3.4. Ice Cover Area**

The reproduction of the sea ice state is among the most complex modeling problems and simultaneously a good diagnostic characteristic, since it reflects the singularities of the atmospheric action and model reproduction of the processes in the upper ocean layer.

Based on the results of several models, the authors of [4] found that the mean annual ice area in the Northern Hemisphere under the specified atmospheric and radiation conditions remains constant when the meridional circulation inherent variability is significant. For our experiment, we present the average sea ice parameters in the Northern Hemisphere for

March and September of 1988–2007, obtained in the considered fifth experimental cycle and in the previous fourth cycle (see Table). The NSIDC satellite data [26] are also shown for comparison. The initial volumes of northern ice in cycles 4 and 5 are almost identical:  $5.9 \times 10^{13}$  and  $6.1 \times 10^{13}$  m<sup>3</sup>. The table indicates that the circulation intensification can be accompanied by a substantial increase in the ice area when the model parameters change, which mainly takes place since ice is more conserved during the summer period. Like in [6], this result contradicts the coupled simulation of the atmosphere, ocean, and ice [27] in which the MHT intensification causes a decrease in the ice area. Such behavior of a stand-alone ocean–ice model

Average areas and trends of March and September ice in the Northern Hemisphere for 1988–2007 according to the INM–IO model and the NSIDC satellite data [26]

Data array	March, million km <sup>2</sup>	March, trend, million km <sup>2</sup> yr <sup>-1</sup>	September, million km <sup>2</sup>	September, trend, million km <sup>2</sup> yr <sup>-1</sup>	MHT at 60° N, PW	MOC, maximum, Sv
Cycle 4	14.95	-0.020	7.51	-0.052	0.22	11
Cycle 5	15.02	-0.006	11.20	-0.024	0.37	21
NSIDC	13.55	-0.042	4.77	-0.075	–	–



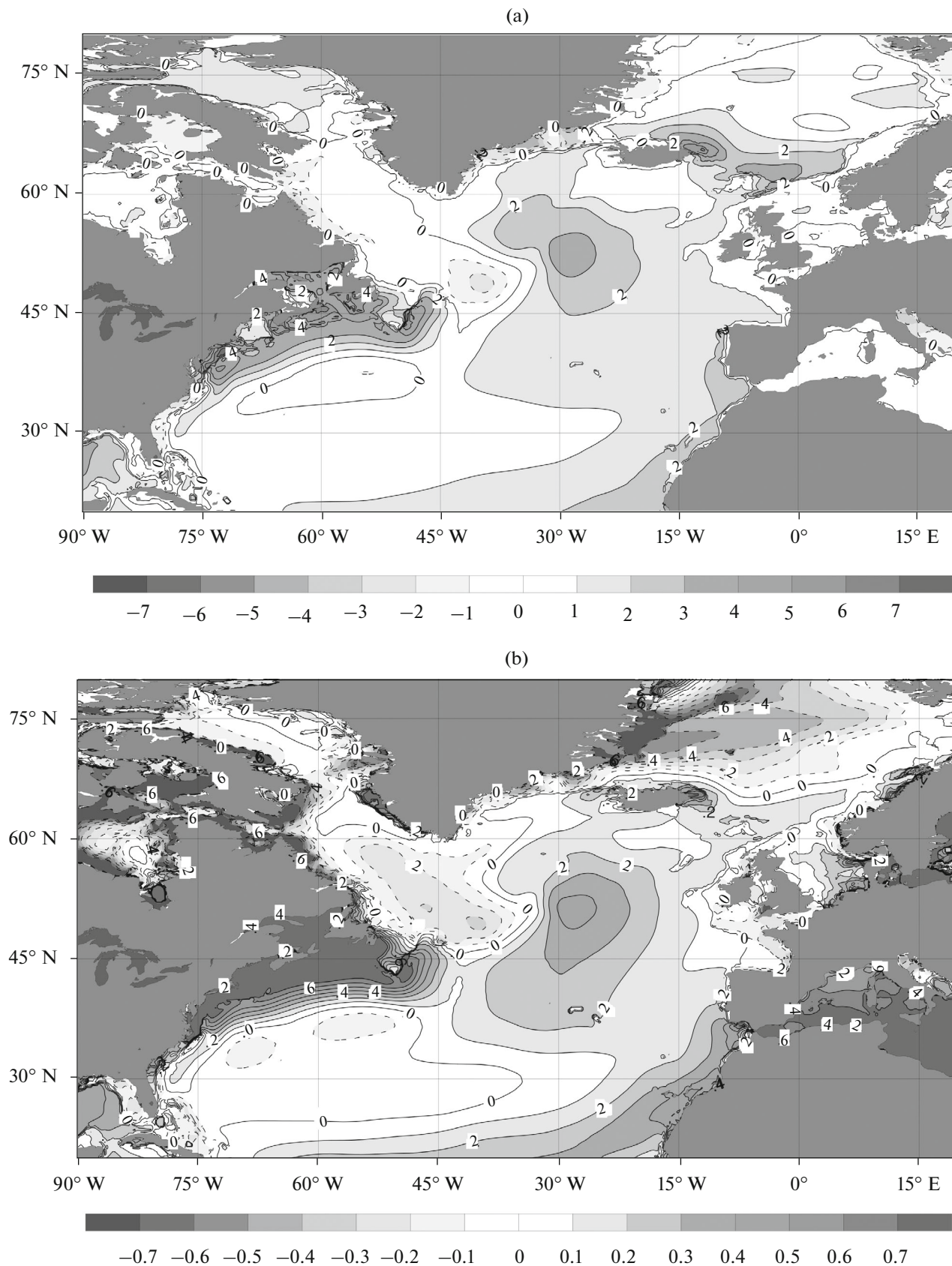


**Fig. 4.** Deviations of (a) temperature ( $^{\circ}\text{C}$ ) and (b) salinity (psu) from the WOA9 mean annual fields averaged over the ocean upper layer with a depth of 700 m.

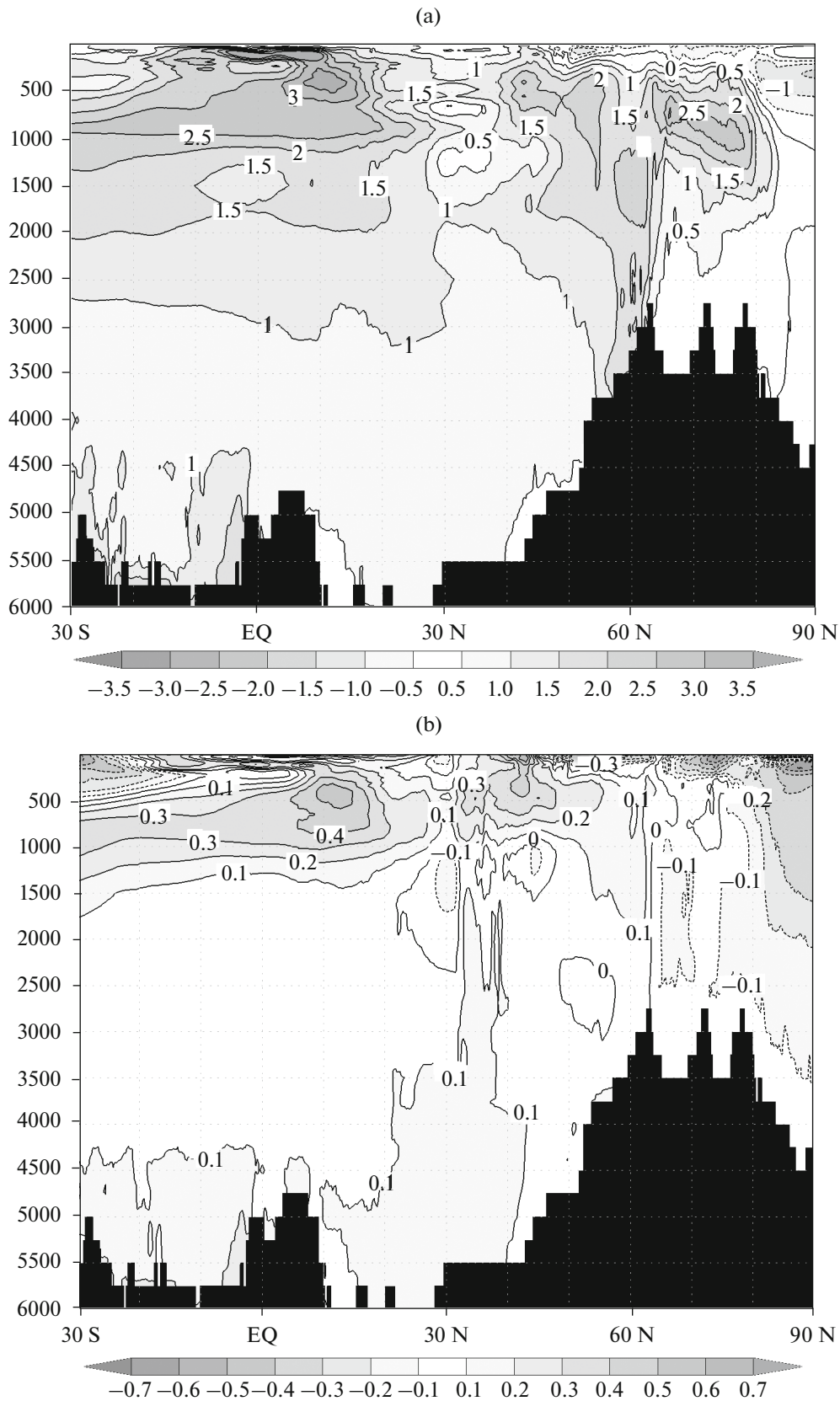


**Fig. 5.** Deviations of (a) temperature ( $^{\circ}\text{C}$ ) and (b) salinity (psu) in the Atlantic Ocean from the WOA09 mean annual fields averaged over latitude.

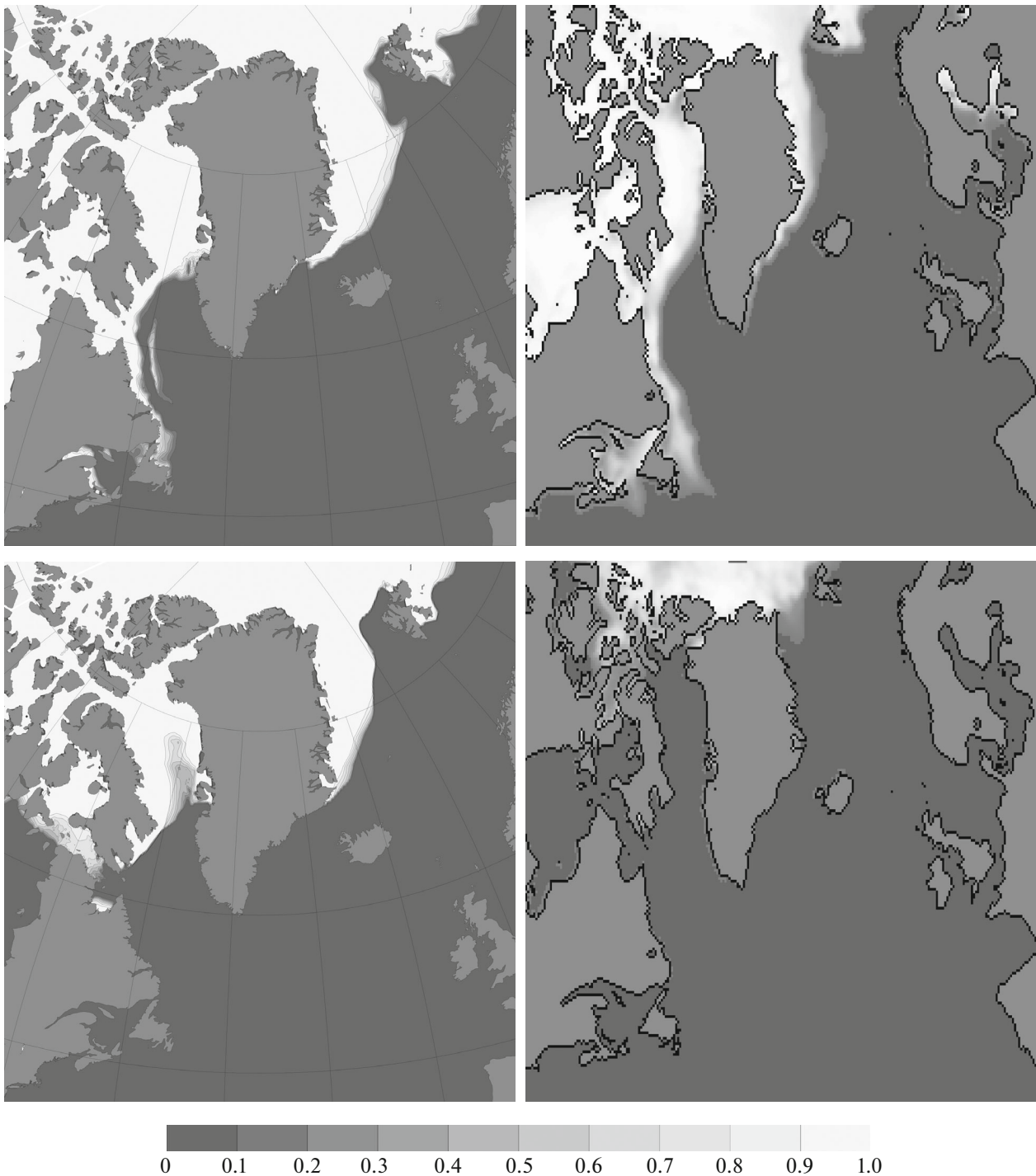


**Fig. 6.** Ice concentration in March (top row) and September (bottom row) in 2007 according to the INM–IO model data (left column) and NSIDC satellite observations (right column).

can be caused by the absence of the feedback with the atmospheric conditions. The origination of a nonrealistic model fluxes near the ice edge in this case is discussed in [4].

To illustrate the experimental results, we present the monthly mean fields of the ice concentration for

March and September 2007 according to the INM–IO model and climatology [26] (Fig. 6). The model qualitatively reproduces the ice area in March except for the Greenland Sea, where the ice concentration is increased. In the Newfoundland region, model ice is on the contrary almost absent, since Gulf Stream



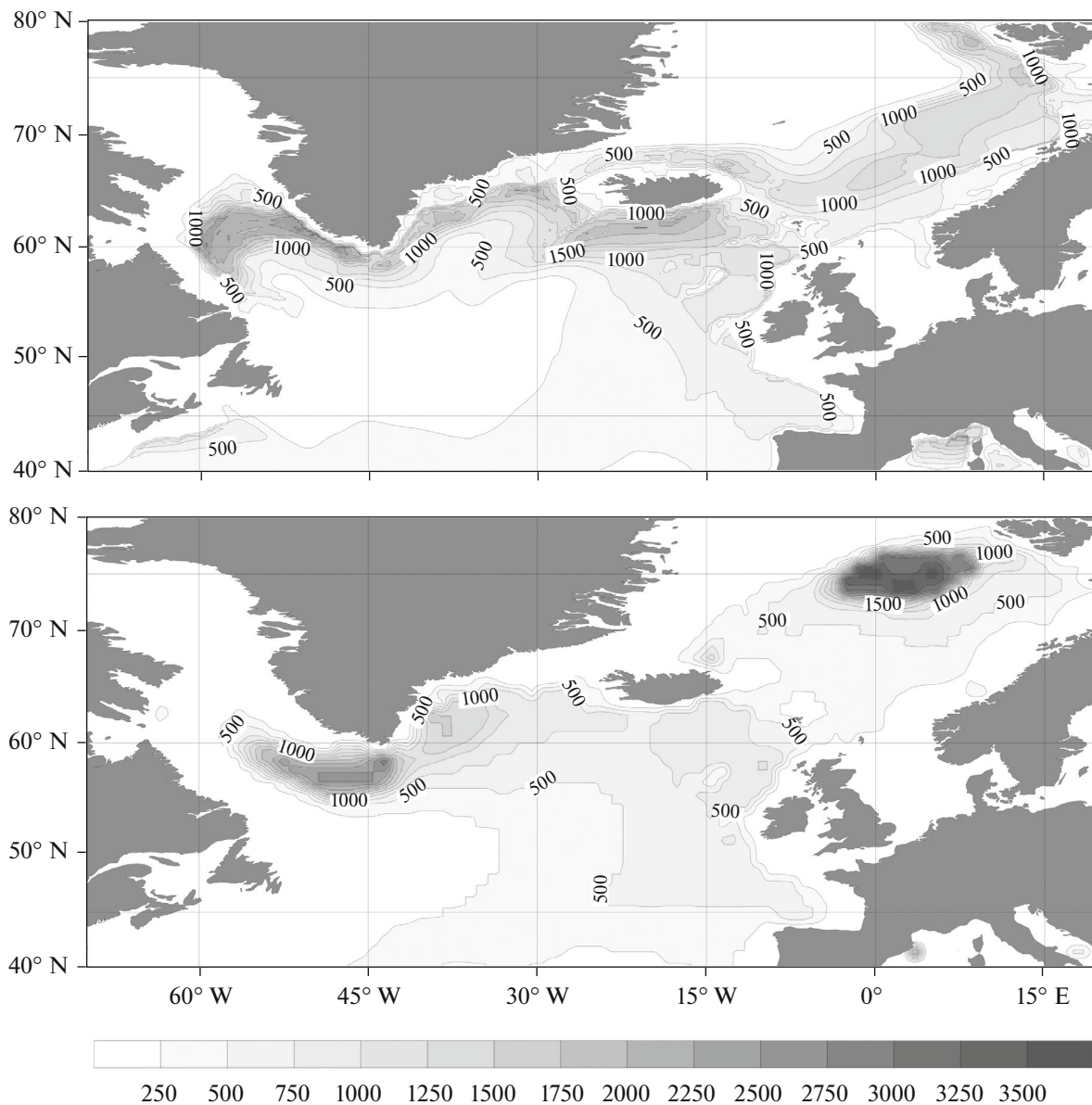


Fig. 7. Average depth of the surface mixed layer in March according to the INM–IO model data (top) and the WOA09 atlas (bottom).

warm water shifts toward the coast. The thermodynamic model [12] substantially increases ice concentration in September due to the accumulation of winter ice, which cannot melt in summer and is not carried by the East Greenland Current into the North Atlantic.

### 3.5. Mixed Layer Depth

The depth distribution in the surface mixed layer (SML) of the ocean is closely related to the formation of deep water and to the heat, fresh water, and carbon dioxide exchange. The deep convection zones in the North Atlantic and the Weddell Sea are among the key elements of the “global ocean conveyor belt.”

Following [6], we consider the March depths of the mixed layer and use the SML determination, according to which the potential density deviation from its surface value in this layer is no more than  $0.125 \text{ kg m}^{-3}$ . For comparison, we construct the SML depth climatic distribution based on the WOA09 March fields of temperature and salinity, taking into account the fact that these depths can be underestimated, since the spatial resolution is low and it is difficult to perform measurements in a cold season.

Figure 7 indicates that the INM–IO model reproduces the deep-water formation boundaries in the Labrador and Irminger seas, as well as the mixing regions in the central North Atlantic. The model generally indicates that mixing at latitudes of  $60^{\circ}$ – $65^{\circ}$  N

is deeper than is shown in the atlas, and the zones of deep SML gravitate toward the shelf slope and are shifted northward. A similar SML depth distribution (specifically, the mixing depths larger than 500 m in the Denmark Strait) was obtained in [6] using the MRI-A model, assimilating the climatic fields of temperature and salinity, and in several works based on the Levitus climatology and the SML determination through a temperature difference, e.g., [28]. Increased mixed layer depths in the Labrador Sea are a typical disadvantage of many up-to-date models [18]. In the Norwegian Sea, mixing depths determined by us are on the contrary pronouncedly decreased, apparently due to the surface fresh anomaly.

#### 4. CONCLUSIONS

This numerical experiment is an important step in the development of the World Ocean model. An analysis of the results indicated that the INM–IO model corresponds to the present-day level of this scientific field development on the considered spatial and time scales. Many detected disadvantages are general for a number of models. The correction methods are proposed for some of these models in the literature and should be found for other models.

Thus, the Atlantic MOC intensity in the INM–IO model solution reaches its maximum far in the north and is on the contrary decreased in the tropics, if the resolution is  $0.25^\circ$  and viscosity is rather high. It is important to correctly reproduce the North Atlantic deep water body. For this purpose, it is apparently necessary to include the parametrization of the bottom water overflow into the model code. It turned out that a decrease in MHT related to large-scale circulation distortions is even a more complex problem.

To all appearance, the deviations from the observational data in the case when the water thermohaline structure is reproduced are first and foremost caused by the incorrect routes of the Gulf Stream and North Atlantic current and weak upwelling in the model solution. It is considered that it is necessary to increase the model resolution in order to correct these disadvantages [4, 18]. The quality of the ice model is of fundamental importance, and the sensitivity of the ocean ice system to the meridional transport intensity should be studied independently.

An analysis of mixed layer depths confirmed the observation [6] that these depths increase at an increased meridional circulation intensity. Buoyancy flows, caused by heat and salt carried from low latitudes, and the effect of flows on the ice cover and, correspondingly, on the heat exchange with the atmosphere can be responsible for this relation. It is necessary to specify the reproduction of the East Greenland Current.

Further works will be related to setting the model in the eddy-permitting regime, improving parametriza-

tions and submodels (in particular, ice and vertical mixing), and transitioning to a higher resolution.

#### ACKNOWLEDGMENTS

We are grateful to Academician A.S. Sarkisyan for consultations and long-term support of this scientific field.

This work was performed at the Institute of Numerical Mathematics, RAS, using the resources of the JSC RAS and Moscow State University supercomputer centers [29], and was supported by the Russian Science Foundation (project no. 14-27-00126).

#### REFERENCES

1. A. S. Sarkisyan, “Fifty years of numerical modeling of baroclinic ocean,” *Izv., Atmos. Ocean. Phys.* **48** (1), 6–20 (2012).
2. A. Sarkisyan and J. Sündermann, *Modelling Ocean Climate Variability* (Springer, Berlin, 2009).
3. R. A. Ibraev, K. V. Ushakov, and R. N. Khabeev, “Eddy-resolving  $1/10^\circ$  model of the World Ocean,” *Izv., Atmos. Ocean. Phys.* **48** (1), 37–46 (2012).
4. S. M. Griffies, A. Biastoch, C. Böning, et al., “Coordinated ocean–ice reference experiments (COREs),” *Ocean Modell.* **26** (1–2), 1–46 (2009).
5. S. M. Griffies, M. Winton, B. Samuels, et al., Datasets and protocol for the CLIVAR WGOMD coordinated ocean–sea ice reference experiments (COREs), WCRP Report No. 21, 2012.
6. G. Danabasoglu, S. G. Yeager, D. Bailey, et al., “North Atlantic simulations in coordinated ocean–ice reference experiments phase II (CORE-II). Part 1: Mean states,” *Ocean Modell.* **73**, 76–107 (2014).
7. World Ocean Atlas 2009. [http://www.nodc.noaa.gov/OC5/WOA09/pr\\_woa09.html](http://www.nodc.noaa.gov/OC5/WOA09/pr_woa09.html).
8. K. V. Ushakov, R. A. Ibraev, and V. V. Kalmykov, “Simulation of the world ocean climate with a massively parallel numerical model,” *Izv., Atmos. Ocean. Phys.* **51** (4), 362–380 (2015).
9. A. V. Gusev and N. A. Diansky, “Numerical simulation of the world ocean circulation and its climatic variability for 1948–2007 using the INMOM,” *Izv., Atmos. Ocean. Phys.* **50** (1), 1–12 (2014).
10. A. S. Sarkisyan, *Numerical Analysis and Prediction of Sea Currents* (Gidrometeoizdat, Leningrad, 1977) [in Russian].
11. V. V. Kalmykov and R. A. Ibraev, “A fast algorithm for solving the system of shallow-water equations on distributed memory computers,” *Vestn. Ufim. Gos. Aviat. Tekh. Univ.* **17** (5), 252–259 (2013).
12. C. Schrum and J. Backhaus, “Sensitivity of atmosphere–ocean heat exchange and heat content in North Sea and Baltic Sea: A comparative assessment,” *Tellus* **51A**, 526–549 (1999).
13. S. M. Griffies and R. W. Hallberg, “Biharmonic friction with a Smagorinsky-like viscosity for use in large-scale eddy-permitting ocean models,” *Mon. Weather Rev.* **128** (8), 2935–2946 (2000).

14. V. V. Kalmykov and R. A. Ibraev, "A framework for the ocean-ice-atmosphere-land coupled modeling on massively-parallel architectures massive-parallel computers," *Vychisl. Metody Program.* **14**, 88–95 (2013).
15. W. Large and S. Yeager, "The global climatology of an interannually varying air–sea flux data set," *Clim. Dyn.* **33** (2–3), 341–364 (2009).
16. J. J.-M. Hirschi, A. T. Blaker, B. Sinha, et al., "Chaotic variability of the meridional overturning circulation on subannual to interannual timescales," *Ocean Sci.* **9** (5), 805–823 (2013).
17. Y. Masumoto, H. Sasaki, T. Kagimoto, et al., "A fifty-year eddy-resolving simulation of the world ocean: Preliminary outcomes of OFES (OGCM for the Earth Simulator)," *J. Earth Simul.* **1**, 35–56 (2004).
18. A. Marzocchi, J. J.-M. Hirschi, N. Holliday, et al., "The North Atlantic subpolar circulation in an eddy-resolving global ocean model," *J. Mar. Syst.* **142**, 126–143 (2015).
19. S. A. Cunningham, T. Kanzow, D. Rayner, et al., "Temporal variability of the Atlantic meridional overturning circulation at 26.5°N," *Science* **317** (5840), 935–938 (2007).
20. A. S. Sarkisyan, *Numerical Analysis and Prediction of Sea Currents* (MGU, Moscow, 2016) [in Russian].
21. R. Dickson and J. Brown, "The production of North-Atlantic deep waters: Sources, rates, and pathways," *J. Geophys. Res.: Oceans* **99** (C6), 12319–12341 (1994).
22. H. Bryden and S. Imawaki, "Ocean heat transport," in *Ocean Circulation and Climate*, Ed. by G. Siedler, J. Church, and J. Gould (Academic, London, 2001), pp. 455–474 (2001).
23. W. E. Johns, M. O. Baringer, and L. M. Beal, "Continuous, array-based estimates of Atlantic Ocean heat transport at 26.5°N," *J. Clim.* **24** (10), 2429–2449 (2011).
24. R. Msadek, W. E. Johns, S. G. Yeager, et al., "The Atlantic meridional heat transport at 26.5°N and its relationship with the MOC in the RAPID array and the GFDL and NCAR coupled models," *J. Clim.* **26** (12), 4335–4356 (2013).
25. S. N. Moshonkin and B. N. Filyushkin, "Influence of bottom gravity currents in gulfs on water masses of North Atlantic," in *Water Masses of Oceans and Seas (Toward the 100-th Anniversary of A. D. Dobrovolskii)* (MAKS press, Moscow, 2007), pp. 130–146 [in Russian].
26. J. Stroeve, Sea ice trends and climatologies from SMMR and SSM/I-SSMIS (updated dataset for 1979–2013), NASA DAAC, Boulder, Colorado, 2003.
27. I. Mahlstein and R. Knutti, "Ocean heat transport as a cause for model uncertainty in projected Arctic warming," *J. Clim.* **24**, 1451–1460 (2011).
28. A. B. Kara, P. A. Rochford, and H. E. Hurlburt, Naval research laboratory mixed layer depth (NMLD) climatologies (2002), NRL Rep. No. BRL/FR/7330-02-9995.
29. V. V. Voevodin, S. A. Zhumatii, S. I. Sobolev, et al., "The Lomonosov supercomputer practice," *Otkrytye Sist.*, No. 7, 36–39 (2012).

*Translated by Yu. Safronov*